

Optical transitions and nature of Stokes shift in spherical CdS quantum dots

D. O. Demchenko and Lin-Wang Wang

Lawrence Berkeley National Laboratory, Berkeley, California 94720

(Dated: October 16, 2018)

We study the structure of the energy spectra along with the character of the states participating in optical transitions in colloidal CdS quantum dots (QDs) using the *ab initio* accuracy charge patching method combined with the folded spectrum calculations of electronic structure of thousand-atom nanostructures. In particular, attention is paid to the nature of the large resonant Stokes shift observed in CdS quantum dots. We find that the top of the valence band state is bright, in contrast with the results of numerous $\mathbf{k}\cdot\mathbf{p}$ calculations, and determine the limits of applicability of the $\mathbf{k}\cdot\mathbf{p}$ approach. The calculated electron-hole exchange splitting suggests the spin-forbidden valence state may explain the nature of the “dark exciton” in CdS quantum dots.

PACS numbers: 73.22.-f, 71.15.Mb, 79.60.Jv

Study of optical properties of semiconductor quantum dots is largely driven by potential applications afforded by their size-dependent bandgap and exciton spectra, such as solar cells,¹ lasers,² and fluorescent tags in biotechnology applications.^{3,4} In addition, quantum dots are excellent testing grounds for the applicability of various theoretical models. One of the most common features of quantum dots is the photoluminescence redshift relative to absorption (also called Stokes shift). There are various causes for the Stokes shift, most common is due to non-resonant absorption in the existence of large size variation in the sample. However even when the non-resonant component has been eliminated, e.g. by the fluorescence line narrowing techniques (FLN) where only the largest quantum dots are excited, there can still exist the Stokes shift. This resonant Stoke shift is usually caused by a dark exciton ground state, but the nature of this dark ground state can vary. A common dark ground state is caused by the exchange interaction between the electron and the hole producing a spin triplet ground state which is spin-forbidden for optical transition.^{5,6} Another possibility consists of the electron and hole having different spatial envelope function symmetries. Since it is relatively rare, this spatial symmetry induced dark exciton ground state has been actively pursued in quantum dots. It has been indicated in previous theoretical and experimental studies that the exciton ground state of a CdS quantum dot is one such candidate.^{7,8} In this work, we will use *ab initio* accuracy calculation to re-investigate this problem.

The use of the $\mathbf{k}\cdot\mathbf{p}$ theory to theoretically investigate the structure of energy levels and exciton states of spherical quantum dots has been very popular.^{9,10,11,12,13,14} It has been shown by various authors, including ourselves, that^{7,8,14} based on the $\mathbf{k}\cdot\mathbf{p}$ calculations, the CdS QDs exciton ground state is an optically passive “dark exciton” for sufficiently small QDs because the hole ground state has an *P*-like envelope function. While the same have been found for CdSe and CdTe quantum dots,¹⁴ the results depend sensitively on the $\mathbf{k}\cdot\mathbf{p}$ parameters used. In contrast, for CdS quantum dots almost all reasonable $\mathbf{k}\cdot\mathbf{p}$

parameters, and even different $\mathbf{k}\cdot\mathbf{p}$ Hamiltonian models (including cubic and wurtzite crystal field splitting) predict the same *P*-like hole ground state, thus indicating the spatial symmetry induced dark exciton. With increasing quantum dot size the hole ground state within the $\mathbf{k}\cdot\mathbf{p}$ framework eventually becomes a bright $1S_{3/2}$ state. This result has seemingly been confirmed by the large values of observed Stokes shift in CdS quantum dots,^{7,8,15,16} the calculated $1P_{3/2}$ - $1S_{3/2}$ splitting values were shown to fit the observed values of resonant Stokes shift.⁷

While the $\mathbf{k}\cdot\mathbf{p}$ model had first successfully predicted the *S*-like state as the VBM in CdSe QDs¹², using a different set of $\mathbf{k}\cdot\mathbf{p}$ parameters generated from the pseudopotential bulk band structure it predicts the *P*-like state as the VBM, in contrast to the direct pseudopotential results¹⁷. This shows that the $\mathbf{k}\cdot\mathbf{p}$ and the pseudopotential methods can predict different S/P ordering for the same set of $\mathbf{k}\cdot\mathbf{p}$ parameters. Unfortunately, the pseudopotential Hamiltonian for CdS quantum dot was previously unavailable, therefore previous theoretical studies on CdS quantum dot have been limited to $\mathbf{k}\cdot\mathbf{p}$ -type calculations or tight-binding calculations.^{7,8,10,15,16,18} Recently, we have developed an *ab initio* accuracy charge patching method. This method can be used to calculate nanosystems of any given semiconductor material. A previous quantum dot/quantum wire calculation using this method for thirteen different semiconductor materials¹⁹ have demonstrated an excellent agreement between the calculated and experimental optical band gaps. Here, we will apply this method to re-investigate the dark exciton problem in CdS quantum dots.

The detailed recipe for our charge patching method calculations is given in Ref. 19, here we only give a briefly outline. The CdS quantum dots are assumed to have wurtzite structure with lattice constants $a = 4.12$ Å and $c = 6.73$ Å. The quantum dot effective radii R_{eff} is determined from estimating the number of atoms in a sphere of radius R_{eff} , assuming equal density of atoms in a quantum dot and the bulk. We are considering quantum dots $(\text{CdS})_{43}$, $(\text{CdS})_{92}$, $(\text{CdS})_{183}$, $(\text{CdS})_{437}$,

$(\text{CdS})_{874}$, $(\text{CdS})_{4586}$ (the subscript is the total number of Cd and S atoms), which have effective radii 6.32 \AA , 8.15 \AA , 10.24 \AA , 13.70 \AA , 17.26 \AA , and 30 \AA respectively. The calculations were performed with the plane-wave pseudopotential method, using local density approximation (LDA) and norm-conserving pseudopotentials. The plane wave energy cut-off of 35 Ry was used in all calculations. A well known LDA shortcoming of underestimating the bandgaps and the electron effective mass was corrected by modifying the nonlocal pseudopotentials (after Ref. 19), such that the electron effective mass in the bulk is in a very good agreement with experiment, i.e. $m_e = 0.213m_0$ calculated here, versus $m_e = 0.210m_0$ measured,²⁰ and the bandgap is partially corrected (it is not possible to correct both simultaneously), i.e. $E_g = 2.16 \text{ eV}$ calculated versus $E_g = 2.58 \text{ eV}$ measured²⁰ (uncorrected LDA yields¹⁹ $m_e = 0.127m_0$ and $E_g = 1.315 \text{ eV}$). Spin-orbit coupling is included and adjusted to yield $\Delta_{SO}=0.068 \text{ eV}$ corresponding to the experimental value.²⁰ In order to eliminate the quantum dot surface dangling bond states and keep the system charge neutral we passivate the surface with pseudo-hydrogen following Ref. 21. A surface atom of valency m is passivated with a pseudo-atom with $Z = (8 - m)/4$, therefore Cd and S are passivated with $\text{H}(Z = 1.5)$ and $\text{H}(Z = 0.5)$, respectively.

The charge patching method²² is used in order to obtain the self-consistent quality real space charge distribution in the quantum dot, without having to perform direct LDA calculations, which for the sizes of the systems considered here are prohibitively expensive. Here, only small prototype systems are computed self-consistently for different atoms and their local environments to generate the motif charge densities. These charge motifs are then used to assemble the total charge density for the entire quantum dot. Knowing the charge density the corresponding LDA potential is generated and the Hamiltonian of a given quantum dot is constructed. The band edge eigenstates of this single particle Hamiltonian are then solved using the folded spectrum method.²³

Our calculated single particle eigenenergies for the valence band are shown in Fig.1. Our calculation produces a $1S_{3/2}$ state as the top of the valence band, and the energies in Fig.1 are plotted relative to this state. For quantum dots in the region of $R_{eff} > 17 \text{ \AA}$ the $1P_{3/2}$ is the second hole state. For smaller quantum dots, there is another $S_{3/2}$ state above the $1P_{3/2}$ state. Even for the largest QD calculated here, i.e. $(\text{CdS})_{4586}$ with effective radius of $R_{eff} = 30 \text{ \AA}$, we do not observe a S-to-P hole groundstate transition, and $1S_{3/2}$ is still a groundstate. On the contrary, the $6 \times 6 \text{ k}\cdot\text{p}$ theory in the spherical approximation, using the effective mass parameters derived from our ab initio bulk band structure ($\gamma_1 = 2.31$, $\gamma_2 = 0.64$, $\gamma_3 = 0.89$, $\Delta_{SO} = 0.068 \text{ eV}$, $E_p = 16.6 \text{ eV}$, $E_g = 2.16 \text{ eV}$, $m_e = 0.21m_0$, and in the spherical approximation $\gamma_{2,3} = 0.79$), yields the $1P_{3/2}$ groundstate, rather than the $1S_{3/2}$ state, as shown in the inset to Fig. 1. For this set of parameters the P-to-S hole groundstate tran-

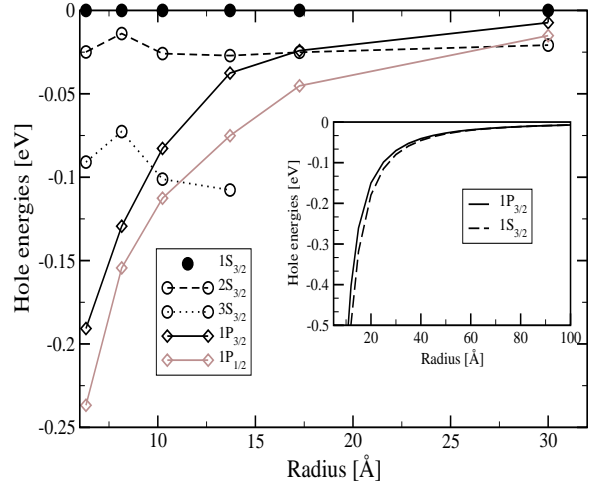


FIG. 1: Size dependence of the valence band energies without electron-hole Coulomb interaction in CdS quantum dots, plotted relative to the top of the valence band, $1S_{3/2}$ state. The inset shows the hole energies of the $1P_{3/2}$ and $1S_{3/2}$ states as a function of the quantum dot size, relative to the bulk valence band maximum, calculated with the spherical $\text{k}\cdot\text{p}$ method. The effective mass parameters used are, $\gamma_1 = 2.31$, $\gamma_2 = 0.79$, and $\Delta_{SO} = 0.068 \text{ eV}$.

sition occurs at the QD effective radius of $\sim 100 \text{ \AA}$. This is similar to other $\text{k}\cdot\text{p}$ calculations even though $\text{k}\cdot\text{p}$ parameters used might be somewhat different.^{7,10,14} (Note, the caption of Fig. 5 in Ref. 7 is in error. The energy is given in the units of $\varepsilon_0 = \gamma_1/(2R^2)$ not $\varepsilon_0 = \gamma_1/(2R)^2$, and the x -axis is $0.529177 \times R(\text{nm})$, not $R(\text{nm})$.) Note, that the $8 \times 8 \text{ k}\cdot\text{p}$ formula should give qualitatively similar results due to the large bandgap. Since the $\text{k}\cdot\text{p}$ predicts $1P_{3/2}$ hole groundstate for $R_{eff} < 100 \text{ \AA}$, our calculations indicate that it is possible that the size range of $\sim 40 \text{ \AA} < R_{eff} < 100 \text{ \AA}$, the $1P_{3/2}$ is indeed the hole groundstate. However, the possible spatial symmetry induced dark exciton in that size range cannot be used to explain the experimentally observed Stokes shift, which is in the range of 15 - 70 meV, while the spatial dark exciton in that size range will have a Stokes shift of 0.6 - 6 meV, as predicted by the $\text{k}\cdot\text{p}$ model. The $\text{k}\cdot\text{p}$ method has been known to predict different ordering (and even omission) of the electronic levels in quantum dots¹⁷ when compared to ab initio pseudopotential method. There has been a debate in the literature as to the proper comparison of the $\text{k}\cdot\text{p}$ and the ab initio methods²⁴. While describing the bulk reasonably well, the two methods can give qualitatively different results when applied to a nanocrystal (for a very detailed study see also Ref. 25). Here we present another particular case of such disagreement.

To compare our results with experimental optical measurements, in addition to the single particle energies, we need to calculate the exciton energies. Exciton energies of optical transitions in the strong confinement regime, where correlation effects are negligible, can be calculated

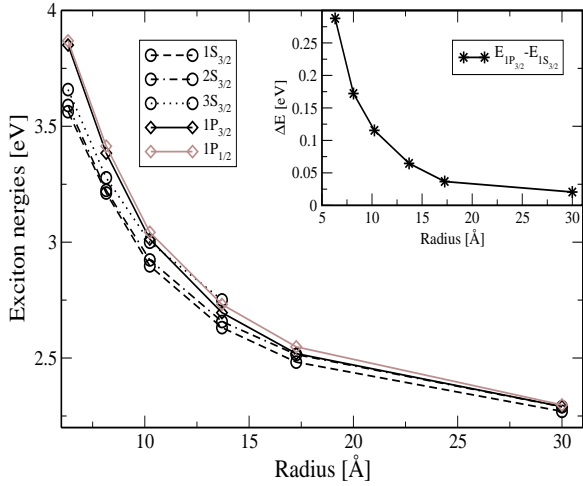


FIG. 2: Size dependence of the energies of excitons constructed from different valence band states including electron-hole Coulomb interaction. The inset shows the energy difference between the $1P_{3/2}$ and $1S_{3/2}$ valence state constructed excitons as a function of the CdS quantum dot size.

from the:

$$E_{ex} = \varepsilon_c - \varepsilon_v - E_{cv}^C - E_{cv}^X, \quad (1)$$

where, ε_c and ε_v are the single-particle conduction and valence states energies, respectively, and E_{cv}^C is the electron-hole Coulomb energy, obtained as²⁶

$$E_{cv}^C = \int \int \frac{|\psi_c(\mathbf{r}_1)|^2 |\psi_v(\mathbf{r}_2)|^2}{\epsilon(\mathbf{r}_1 - \mathbf{r}_2) |\mathbf{r}_1 - \mathbf{r}_2|} d\mathbf{r}_1 d\mathbf{r}_2 \quad (2)$$

where, $\mathbf{x} \equiv (\mathbf{r}, \sigma)$ includes both spatial \mathbf{r} and spin $\sigma = \uparrow, \downarrow$ variables, $\epsilon(\mathbf{r}_1 - \mathbf{r}_2)$ is a position-dependent dielectric function (described below), and $\psi_c(\mathbf{x})$ and $\psi_v(\mathbf{x})$ are the wavefunctions for the conduction and valence states, respectively. The exciton energies can be further split by the electron-hole exchange interaction E_{cv}^X in Eq.(1). The exchange integral E_{cv}^X is calculated as:

$$E_{cv}^X = \int \int \frac{\psi_v^*(\mathbf{x}_1) \psi_c^*(\mathbf{x}_2) \psi_c(\mathbf{x}_1) \psi_v(\mathbf{x}_2)}{\epsilon(\mathbf{r}_1 - \mathbf{r}_2) |\mathbf{r}_1 - \mathbf{r}_2|} d\mathbf{r}_1 d\mathbf{r}_2. \quad (3)$$

In using the model dielectric function $\epsilon(\mathbf{r}_1 - \mathbf{r}_2)$ we follow the procedure outlined in Ref. 27, where the short range exchange interaction is essentially unscreened while the long range exchange interaction is screened significantly. Note that, to get the exchange splitting of the exciton energy, Eq.(1) needs to be diagonalized among a few Kramers doublet spin configurations, which are degenerate under the first three terms in Eq.(1).

The calculated exciton energies using Eq.(1) without the E_{cv}^X term are shown in Fig.2. The inset to Fig.2 shows the $1S_{3/2}$ and $1P_{3/2}$ energy difference which include electron-hole Coulomb interaction as a function of the QD radius. The $E_{1P_{3/2}} - E_{1S_{3/2}}$ difference for the exciton has been enlarged compared to the single particle

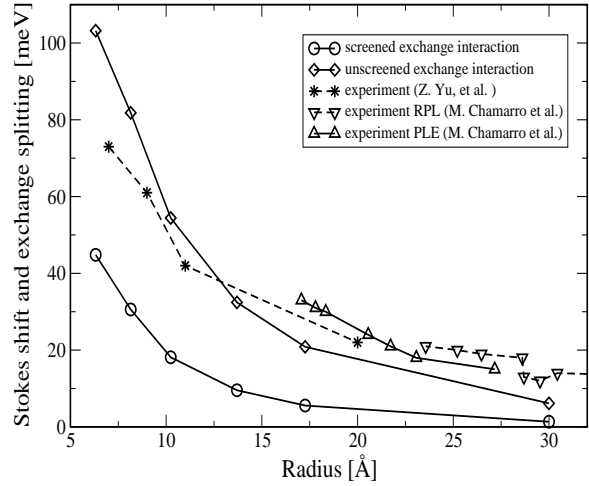


FIG. 3: Electron-hole exchange splitting in comparison with experimentally measured resonant Stokes shift. Experimental data is deduced from Ref.7 (Z. Yu et al.) and from Ref.18 (M. Chamorro et al.), measured with resonant photoluminescence (RPL) and photoluminescence excitation (PLE).

energies. This is because the $1S_{3/2}$ hole state has larger Coulomb interaction energy with the electron than the $1P_{3/2}$ hole. Indeed, in the literature, there are reports of order changing in exciton states due to this Coulomb energy difference.¹⁵ In our case, it just makes the P -like hole state dark exciton less likely.

We then add in the exchange interaction, and calculate the exciton exchange splitting for our calculated $1S_{3/2}$ hole ground state exciton, therefore producing a spin-forbidden dark exciton. While there is no debate about the screening in the electron-hole Coulomb interaction, there exists a controversy regarding screening of the electron-hole exchange interaction in excitons. For example, when calculating optical properties in Si quantum dots²⁸ and hydrogenated Si clusters²⁹ authors have calculated exciton energy structure with unscreened exchange interaction, following the argument that in the Bethe-Salpeter equation³⁰ for the excitonic state the exchange term should be unscreened, otherwise leading to improper diagrams. Recently, however, it was shown³¹ that when the two-particle Green's function is constructed from a small set of particle-hole states, it may be appropriate to screen the electron-hole exchange interaction. Therefore, in this work, along with the screened electron-hole exchange splitting we also calculate unscreened exchange splitting for comparison.

The results are summarized in Fig. 3, where we plot the singlet-triplet exciton energy splitting for the screened exchange interaction, unscreened exchange interaction, and experimental data taken from Refs. 7 and 18. The overall trend of the electron-hole exchange splitting agrees with the experimental data for the resonant Stokes shift. The experiment seems to favor the unscreened electron-hole exchange splitting results. This is in agreement with a previous tight-binding study¹⁸ where

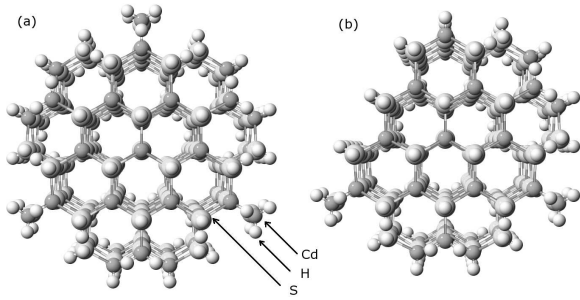


FIG. 4: Symmetric (a) and asymmetric (b) CdS quantum dots. The asymmetric dots exhibit a much (two orders of magnitude) smaller radiative lifetimes for P-type hole states, compared with symmetric dots.

the exchange interaction was also unscreened. On the other hand, there is a systematic discrepancy between the experiment and calculated values of the screened electron-hole exchange splitting. Overall, our results indicate that singlet-triplet splitting could be responsible for the observed values of the resonant Stokes shift in the experiment. In order to confirm this theoretical prediction we propose an experiment in which the resonant Stokes shift is measured as a function of applied external magnetic field. The linear dependence of the Zeeman splitting on the external magnetic field could be detected from the Stokes shift measurement.⁵

Last, to further study the possibility of the *P*-like hole induced spatial dark exciton, we have examined the geometry dependence of the spatial dark exciton radiative life time. Note that the quantum dot (wurtzite) structures considered so far are highly symmetric. Namely, there is a 120 degree rotation symmetry along the dot center *z*-axis (looking down in Fig. 4). However, quantum dots obtained in experiment will always have some structural imperfections, away from the perfect symmetric shape. It is therefore interesting to study the influence of such imperfection on the rate of optical transitions. Here we calculate radiative lifetimes τ , following Ref. 32. Experimentally measured values for the radiative lifetimes are⁷ ~ 180 ns for the slow component of

the luminescence at the temperature of 10 K which corresponds to the radiative recombination of the optically passive state. In our calculations for the symmetric quantum dot [Fig.4(a)] we obtain radiative lifetimes of 1 ns for *S*-like states, and very long (> 1000 ns) lifetime for *P*-like states, the latter is at least an order of magnitude larger than observed in experiment. We then calculated a similar sized quantum dot with its axial symmetry removed [Fig.4(b)]. As a result, the radiative lifetime of the dark $1P_{3/2}$ induced exciton decreases sharply to ~ 20 ns, much smaller than the observed experimental lifetime. Since it is hard to expect perfect symmetric structures in the experiment, this result further supports the idea that the experimentally observed Stoke shift is not caused by the spatial dark exciton, rather it might be caused by the exchange interaction induced spin-forbidden dark exciton. Note that the spin-forbidden dark exciton will not be eliminated by the change of spatial shape of the quantum dot, and the CdS experimental lifetime of ~ 180 ns (DQ of $R = 11$ Å at $T = 10$ K) is similar to the dark exciton lifetime in CdSe (210 ns for DQ of $R = 13$ Å at $T = 12$ K)³³ where it is known that the dark exciton is caused by the exchange splitting.

In summary, we have performed calculations of exciton states, optical properties, and electron-hole exchange splitting in CdS quantum dots. The results indicate that the previous $\mathbf{k}\cdot\mathbf{p}$ method wrongly assigned the top of valence band for small ($R_{eff} < 30$ Å) CdS quantum dots. Our hole ground state is found to be bright *S*-state, rather than dark *P*-state predicted by the $\mathbf{k}\cdot\mathbf{p}$ method. As a consequence, the dark exciton is not spatially forbidden in CdS quantum dot. Our calculation indicates that the exchange splitting might be responsible for the dark exciton and the observed Stoke shift. We recommend the magnetic field experiments to further resolve this issue.

We would like to thank Joshua Schrier for helping with the charge patching code, Byoung hak Lee for useful discussions. This work was supported by the Director, Office of Energy Research, Office of Science, and Division of Material Science, of the U.S. Department of Energy under Contract No. DE-AC02-05CH11231. It used the resources of National Energy Research Scientific Computing Center (NERSC).

¹ I. Gur, N. A. Fromer, M. L. Geier, and A. P. Alivisatos, *Science* **310**, 462 (2005).

² M. Acherman, M. A. Petruska, S. Kos, D. L. Smith, D. D. Koleske, V. I. Ekimov, *Nature* **429**, 642 (2004).

³ J. K. Jaiswal, E. R. Goldman, H. Mattoissi, and S. M. Simon, *Nature Methods*, **1**, 73 (2004).

⁴ W. Chan, S. Nice, *Science* **281**, 2016 (1998).

⁵ M. Nirmal, D. J. Norris, M. Kuno, M. G. Bawendi, Al. L. Efros, and M. Rosen, *Phys. Rev. Lett.* **75**, 3728 (1995).

⁶ Al. L. Efros, M. Rosen, M. Kuno, M. Nirmal, D. J. Norris, and M. Bawendi, *Phys. Rev. B* **54**, 4843 (1996).

⁷ Z. Yu, J. Li, D. B. O'Connor, L. W. Wang, P. F. Barbara,

J. Phys. Chem. B **107**, 5670 (2003).

⁸ J. Li and J. B. Xia, *Phys. Rev. B* **62**, 12613 (2000).

⁹ Al. L. Efros and A. V. Rodina, *Solid State Commun.* **72**, 645 (1989).

¹⁰ G. B. Grigoryan, E. M. Kazaryan, Al. L. Efros, and T. V. Yazeva, *Sov. Phys. Solid State* **32**, 1031 (1990).

¹¹ J. B. Xia, *Phys. Rev. B* **40**, 8500 (1989).

¹² A. I. Ekimov, F. Hache, M. C. Schanne-Klein, D. Ricard, C. Flytzanis, I. A. Kudryavtsev, T. V. Yazeva, A. V. Rodina, Al. L. Efros, *J. Opt. Soc. Am. B* **10**, 100 (1993).

¹³ J.-B. Xia and J. Li, *Phys. Rev. B* **60**, 11540 (1999).

¹⁴ T. Richard, P. Lefebvre, H. Mathieu, and J. Allègre, *Phys.*

Rev. B **53**, 7287 (1996).

¹⁵ V. A. Fonoberov, E. P. Pokatilov, and A. A. Balandin, Phys. Rev. B **66** 085310 (2002).

¹⁶ G. W. Bryant and W. Jaskolski, Phys. Rev. B **67**, 205320 (2003).

¹⁷ L. W. Wang and A. Zunger, J. Phys. Chem. B **102**, 6449 (1998).

¹⁸ M. Chamarro, M. Dib, V. Voliotis, A. Filoromo, P. Rousignol, T. Gacoin, J. P. Boilot, C. Delerue, G. Allan, and M. Lannoo, Phys. Rev. B **57**, 3729 (1998).

¹⁹ J. Li and L. W. Wang, Phys. Rev. B **72**, 125325 (2005).

²⁰ *Semiconductors: Data Handbook*, 3rd ed., edited by O. Madelung (Springer-Verlag, Berlin, 2004).

²¹ L. W. Wang and J. Li, Phys. Rev. B **69**, 153302 (2004).

²² L. W. Wang, Phys. Rev. Lett. **88**, 256402 (2002).

²³ L. W. Wang and A. Zunger, J. Chem. Phys. **100**, 2394 (1994).

²⁴ H. Fu, L.-W. Wang, and A. Zunger, Appl. Phys. Lett. **71**, 3433 (1997); **73**, 1157 (1998); Al. L. Efros and M. Rosen, Appl. Phys. Lett. **73**, 1155 (1998).

²⁵ H. Fu, L.-W. Wang, and A. Zunger, Phys. Rev. B **57**, 9971 (1998).

²⁶ A. Franceschetti and A. Zunger, Phys. Rev. Lett. **78**, 915 (1997).

²⁷ A. Franceschetti, L. Wang, H. Fu, and A. Zunger, Phys. Rev. B **58**, R13367 (1998).

²⁸ T. Takagahara and K. Takeda, Phys. Rev. B **53**, R4205 (1996).

²⁹ M. Rohlffing and S. G. Louie, Phys. Rev. Lett. **80**, 3320 (1998).

³⁰ L. J. Sham and T. M. Rice, Phys. Rev. **144**, 708 (1966).

³¹ L. X. Benedict, Phys. Rev. B **66**, 193105 (2002).

³² L. W. Wang and A. Zunger, J. Phys. Chem. **98**, 2158 (1993).

³³ S. A. Crooker, T. Barrick, J. A. Hollingsworth, and V. I. Klimov, Appl. Phys. Lett. **82**, 2793 (2003).